First principles study of structural, electronic and optical properties of AgSbS2

ARTICLE *in* MATERIALS SCIENCE IN SEMICONDUCTOR PROCESSING · NOVEMBER 2013

Impact Factor: 1.96 · DOI: 10.1016/j.mssp.2013.04.009

4 AUTHORS, INCLUDING:

Saadi Berri
University of Setif, 19000 Setif, Algeria
16 PUBLICATIONS **46** CITATIONS
SEE PROFILE

D. Maouche
Ferhat Abbas University of Setif
47 PUBLICATIONS **263** CITATIONS
SEE PROFILE

Youcef Medkour
University of Setif 1,Setif, Algeria
26 PUBLICATIONS **74** CITATIONS
SEE PROFILE

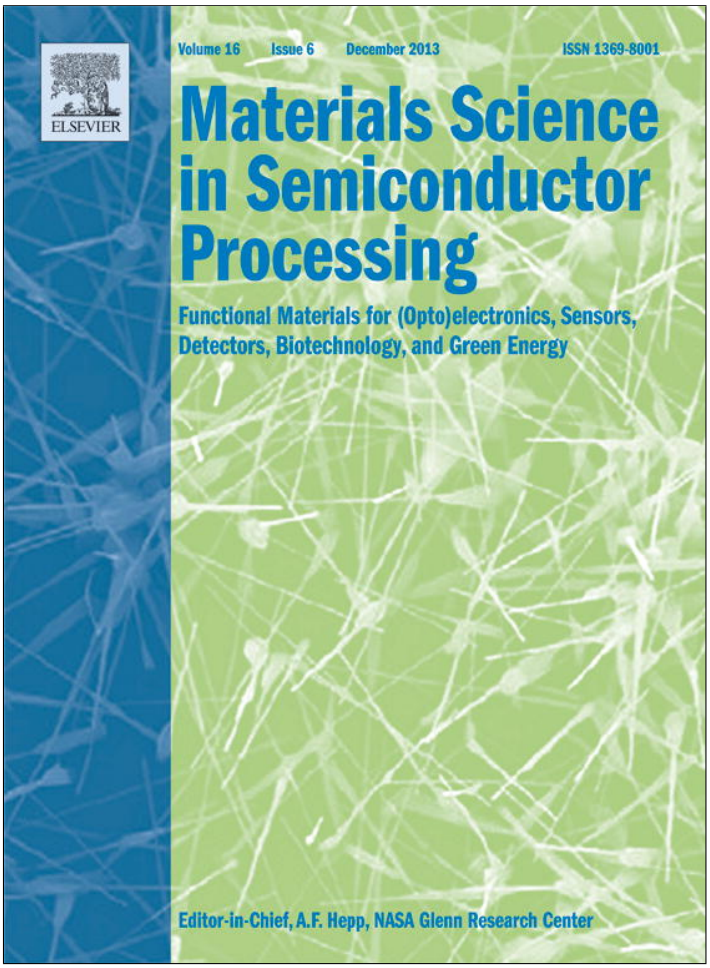

Materials Science in Semiconductor Processing 16 (2013) 1439–1446

Contents lists available at SciVerse ScienceDirect

Materials Science in Semiconductor Processing

journal homepage: www.elsevier.com/locate/mssp

Review

First principles study of structural, electronic and optical properties of $AgSbS_2$

Saadi Berri [a,*], D. Maouche [b], N. Bouarissa [c], Y. Medkour [a]

[a] Department of Physics, Faculty of Science, University of Setif, 19000 Setif, Algeria
[b] Laboratory for Developing New Materials and their Characterizations, University of Setif, 19000 Setif, Algeria
[c] Department of Physics, College of Science and Arts and Centre for Advanced Materials and Nano-Research (CAMNR), Najran University, Najran 11001, Saudi Arabia

ARTICLE INFO

Available online 5 July 2013

Keywords:
FP-LAPW
PP-PW
Electronic structure
Phase transition
Optical properties

ABSTRACT

In this work, we study the structural, electronic and optical properties of $AgSbS_2$, using full-potential linearized augmented plane wave and the pseudopotential plane wave scheme in the frame of generalized gradient approximation. Features such as the lattice constant, bulk modulus and its pressure derivative are reported. Our results suggest a phase transition from AF-IIb phase to rocksalt (B1) phase under high pressure. The calculated band structure and density of states show that the material under load has an indirect energy band gap $X \rightarrow (L\Gamma)$ for AF-IIb phase (semiconductor) and a negative band gap $W \rightarrow (\Gamma X)$ for B1 phase (semimetal). The optical properties are analyzed and the origin of some peaks in the spectra is discussed. Besides, the dielectric function, refractive index and extinction coefficient for radiation up to 14 eV have also been reported and discussed.

Contents

1. Introduction

Recently the ABX_2 type compounds have attracted attention due to their potential applications as solar cells and non-linear optical devices. They have been found to undergo phase transitions under pressure effect [1–5]. More complex chalcogenides, e.g., ternary and quaternary have also been proposed for thermoelectric applications [6–10].

$AgXS_2$ sulphosalts (in which X is As, Bi or Sb) are a group of semi-conducting sulfides that occur naturally as minor components of polymetallic sulfide ores [11]. Many heavy chemical elements have multiple valence states and complex bonding arrangements in crystal structures that are poorly understood [12]. In addition to these relatively low-temperature, naturally occurring phases, synthetic high-temperature polymorphs exist, forming a complex

* Corresponding author. Tel.: +213 95115576; fax: +213 36 92 72 10.
E-mail address: berrisaadi12@yahoo.fr (S. Berri).

1369-8001/$ - see front matter © 2013 Elsevier Ltd. All rights reserved.
http://dx.doi.org/10.1016/j.mssp.2013.04.009

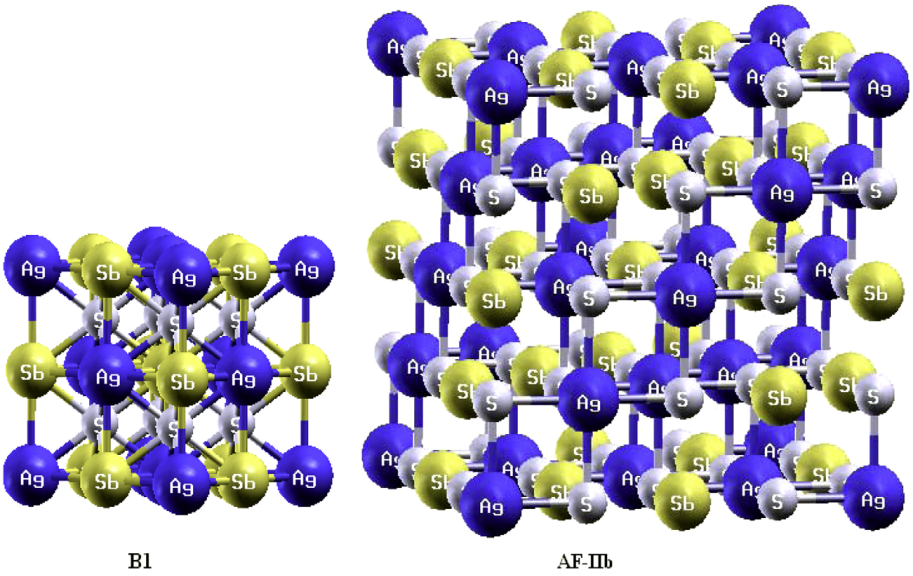

Fig. 1. Crystal structure of AF-IIb and B1 phases of $AgSbS_2$ compound.

group of compounds all of which can be considered in terms of the fcc galena structure but which also display lower-symmetry derivatives [11]. It is known that $AgSbS_2$ crystallizes in the B1 structure under high pressure effect. Nevertheless, to the best of our knowledge, there are no previous studies on AF-IIb phase. The ordering of Ag and Sb on a face-centred cubic (fcc) lattice has been confirmed recently [13].

Miargyrite, $AgSbS_2$, was chosen for detailed study because it contains medium-heavy elements suitable for pioneering new synchrotron X-ray techniques in diffraction and absorption spectroscopy [12]. Generally, the material $AgSbS_2$ is widely used for important technical and device applications. It is found to be excellent candidate for the fabrication of optical frequency converters in solid-state laser systems [14], photovoltaic applications [15] and development of solar cells [16–18].

In the present paper, the structural, electronic and optical properties of $AgSbS_2$ are reported. As far as the electronic structure and optical properties of materials are concerned, these features play a crucial role in determining their opto-electronic properties for devices. Therefore, accurate knowledge of these properties is very important for the application. The aim of this work is to examine the electronic band structure of $AgSbS_2$, with emphasis on its derived properties. The calculations are performed using ab initio full-potential linearized augmented plane wave (FP-LAPW) and the pseudopotential plane wave (PP-PW) within the density functional theory (DFT) with the generalized gradient approximation (GGA). The used methods are described in Section 2, whereas the results regarding the structural, electronic and optical properties are presented and discussed in Section 3. Finally, a summary of our results is given in Section 4.

2. Computational method

The first principles calculations were performed by employing FP-LAPW approach [19], based on the DFT [20] as implemented in WIEN2K code [21]. The Kohn–Sham equations are solved self-consistently using the FP-LAPW method. In the calculations reported here, we use a parameter $R_{MT}K_{max}=9$, which determines matrix size (convergence), where K_{max} is the plane wave cut-off and R_{MT} is the smallest of all atomic sphere radii. We have chosen the muffin-tin radii (MT) for Ag, Sb, and S to be 2.2, 2.3 and 2 (a.u), respectively. Exchange–correlation effects are treated using GGA as parameterized by Perdew et al. [22]. Self-consistent calculations are considered to be converged when the total energy of the system is stable within 10^{-4} Ry. The convergence criteria for total energy and force are taken as 10^{-5} and 10^{-4} eV/Å, respectively. The valence wave functions inside the spheres are expanded up to $l_{max}=10$ while the charge density was Fourier expanded up to $G_{max}=14$. The Monkorst–Pack special k-points were performed using 47 special k-points in the irreducible Brillouin zone for B1, and 20 k-points for the AF-IIb phase [23]. Calculations of the frequency-dependence of the optical properties were carried out using 256 and 195 k-points for the B1 and AF-IIb phases, respectively.

Optical properties of a solid are usually described in terms of the complex dielectric function $\varepsilon(w)=\varepsilon_1(w)+i\varepsilon_2(w)$. The imaginary part $\varepsilon_2(w)$ was calculated from the momentum matrix elements between the occupied and unoccupied wave functions within the selection rules. The real part $\varepsilon_1(w)$ of the dielectric function was calculated by the Kramers–Kronig transformation [24] of the imaginary part $\varepsilon_2(w)$. Other optical constants were computed from the values of $\varepsilon_1(w)$.

We have used the norm-conserving pseudopotential (NCP) method [25] and the GGA approach according to Perdew–Burke–Ernzerhof [22]. A computer program CASTEP (Cambridge Serial Total Energy Package) [26], was used to calculate structural, electronic and optical properties of $AgSbS_2$. The kinetic cut-off energy for the plane wave expansion is taken to be 500 eV for all cases. The special points sampling integration over the Brillouin

zone was employed by using the Monkhorst–Pack method with $7 \times 7 \times 7$ k-points for B1 and $4 \times 4 \times 4$ k-point for the AF-IIb phase [23]. Based on the Broyden Fletcher Goldfarb Shenno (BFGS) [27] minimization technique, the system reached the ground state via self consistent calculation when the total energy is stable to within 5×10^{-6} eV/atom, and less than 10^{-2} eV/Å for the force.

To calculate the optical properties, dense Monkorst–Pack special k-points were used. $14 \times 14 \times 14$ for B1, and $8 \times 8 \times 8$ special k-points mesh for the AF-IIb phase [23]. The crystal structure of B1 and AF-IIb phases are shown in Fig. 1.

3. Results and discussion

3.1. Structural properties

Our basic procedure in this work is to calculate the total energy as a function of the unit-cell volume around the equilibrium cell volume V_0 in both AF-IIb and B1 phases, using FP-LAPW and PP-PW methods. We present, in Fig. 2, structural optimization curves obtained by using the FP-LAPW method in both phases, and the data are fitted to the Murnaghan's equation of state [28] so as to determine the ground state properties, such as equilibrium lattice constant a, bulk modulus B and its pressure derivative B'. The calculated structural parameters of $AgSbS_2$ are summarized in Table 1. Note that our FP-LAPW result regarding the lattice constant for the B1 phase deviates from the experimental value reported in Ref. [29] by about 3% whereas that obtained by PW-PP for the same phase deviates by about 19%. The calculated lattice parameter by FP-LAPW is in better agreement with the experiment compared to that obtained by PP-PW. Nevertheless, both used methods overestimated the lattice constant with respect to experiment. This is not surprising, the results are consistent with the general trend of the GGA approach [30,31]. To our knowledge, there are no experimental or theoretical data reported for the bulk modulus and its pressure derivative for the material of interest, and hence our results are predictions. We have also included in Table 1 the bulk modulus and its pressure derivative B' values for Co_2CrBi [32] and Pd_2ZrAl, Pd_2ZrIn, Pd_2HfAl and Pd_2HfIn [33] for comparison purpose. Note that the bulk modulus for B1 phase obtained by the FP-LAPW method deviates from that obtained by the PP-PW method by about 5%, whereas for AF-IIb phase the deviation is less than 9%. Almost the same conclusion can be drawn for the pressure derivative of the bulk modulus (B'). We observe that the bulk modulus of the B1 phase of $AgSbS_2$ is larger than that of AF-IIb phase. This could be traced back to the difference in bond lengths between the two structures. On the other hand, the bulk modulus of Co_2CrBi, Pd_2ZrAl, Pd_2ZrIn, Pd_2HfAl and Pd_2HfIn materials seems to be much larger than that of $AgSbS_2$ in both phases being considered here. This suggests that $AgSbS_2$ is less compressible than those materials.

It is obvious that AF-IIb phase is more stable. Our FP-LAPW and PP-PW results showed that AF-IIb phase of the material under load transforms to the rocksalt (B1) phase at pressures of 15.5 and 31.3 GPa, respectively. This has

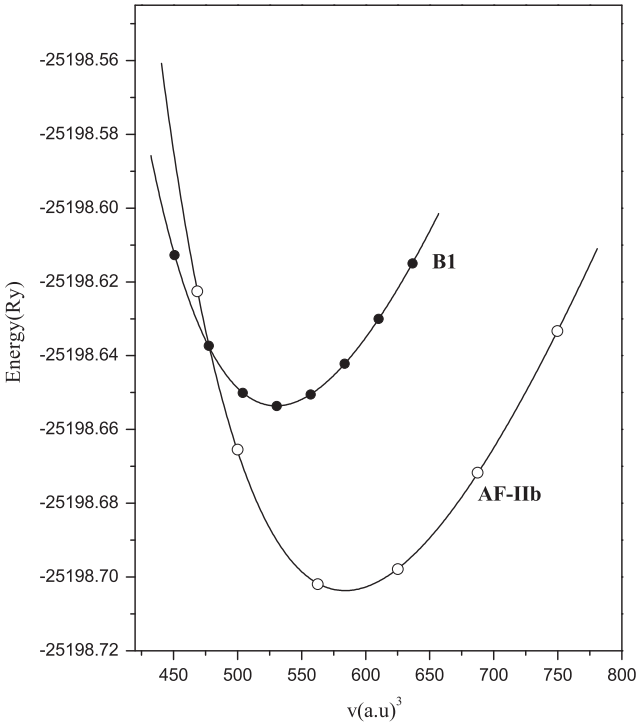

Fig. 2. Calculated total energy as a function of volume in the AF-IIb and B1 structure for $AgSbS_2$.

Table 1
Lattice constant a (Å), bulk modulus B (in GPa) pressure derivative of bulk modulus B' for $AgSbS_2$.

			Present work (FP-LAPW)	Present work (PW-PP)	Experiment
$AgSbS_2$	AF-IIb	a	11.15	11,05	–
		B	68.315	74.31	–
		B'	4.58	4.25	–
	B1	a	5.83	6.72	5.647 [29]
		B	73.85	77.87	–
		B'	4.73	4.33	–
Co_2CrBi [32]		B	132.7	–	–
		B'	5.20	–	–
Pd_2ZrAl [33]		B	151	–	–
Pd_2ZrIn [33]		B	141	–	–
Pd_2HfAl [33]		B	159	–	–
Pd_2HfIn [33]		B	150	–	–

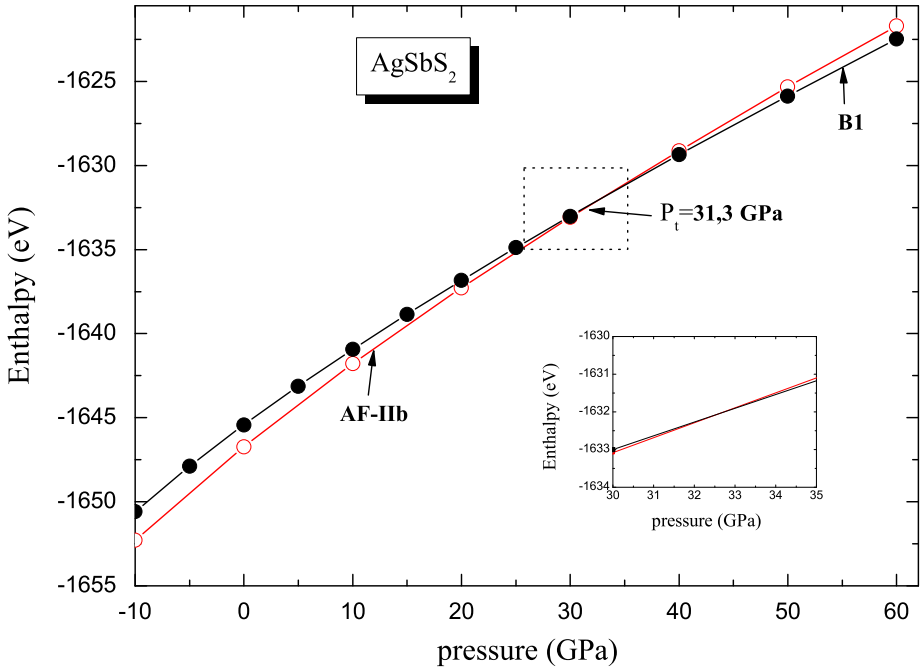

Fig. 3. Pressure vs. enthalpy plot for $AgSbS_2$ compound.

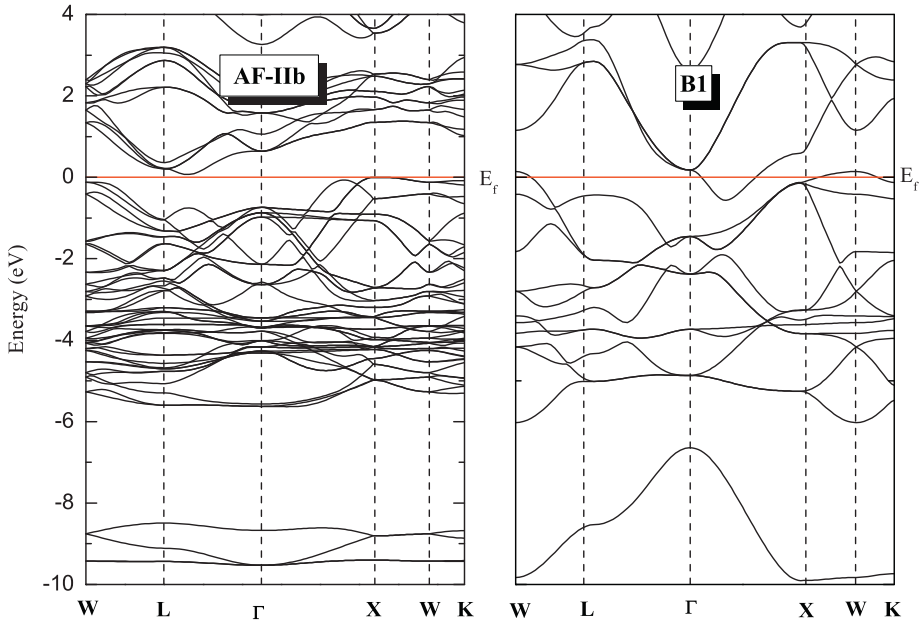

Fig. 4. Band structure for high-symmetry directions in the Brillouin zone of $AgSbS_2$ for AF-IIB and B1 structure.

been done by calculating the Gibbs free energy (G), ($G=E_0+PV-TS$) for the two phases of interest and assuming zero temperature (frozen ionic degree of freedom). At zero temperature, the Gibbs free energy becomes equal to the enthalpy, i.e. $H=E_0+pV$. Thus, in the absence of any barrier, a transition occurs when the enthalpy of the lower-pressure phase equals that for some other structure, which becomes the stable phase above this coexistence pressure [34]. The transition pressure is obtained from the enthalpy curve crossings. The diagram that represents pressure vs. enthalpy is plotted in Fig. 3 which allowed the determination of the transition pressure. As mentioned above, the transition pressure obtained by FP-LAPW differs largely from that obtained by PP-PW. The difference is believed to be due to the used methods. In the absence of the experimental data regarding the transition pressure of the material of interest, no comment can be ascribed to the accuracy of these two methods.

3.2. *Electronic properties.*

The band structures of $AgSbS_2$ have been calculated at the theoretical equilibrium lattice constant for AF-IIb and B1 structures using both FP-LAPW and PP-PW methods. Because of the similarity in the most results, only FP-LAPW results are presented. The energy band structure,

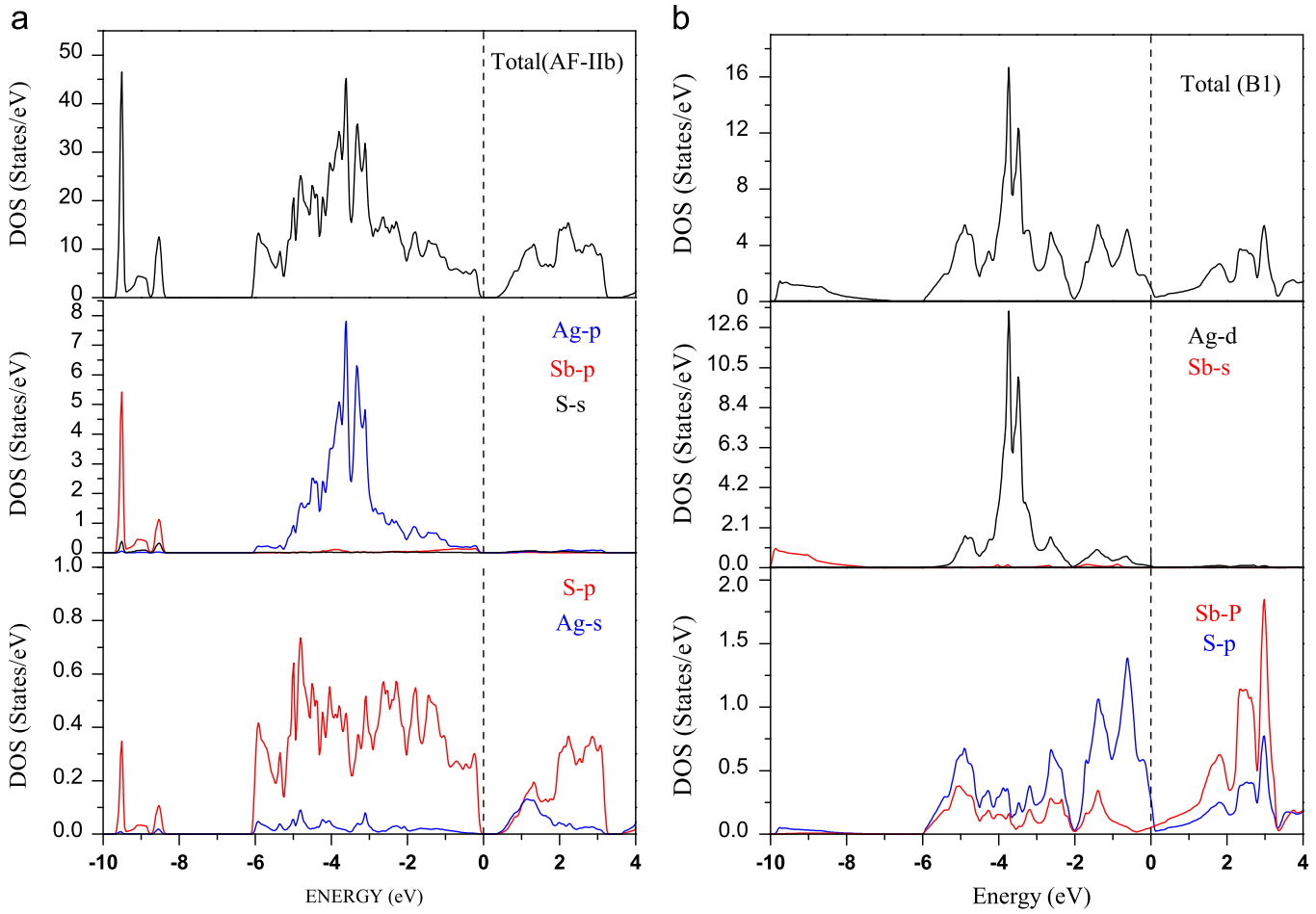

Fig. 5. Total and partial DOS of $AgSbS_2$ for (a)AF-IIb and (b) B1 structures.

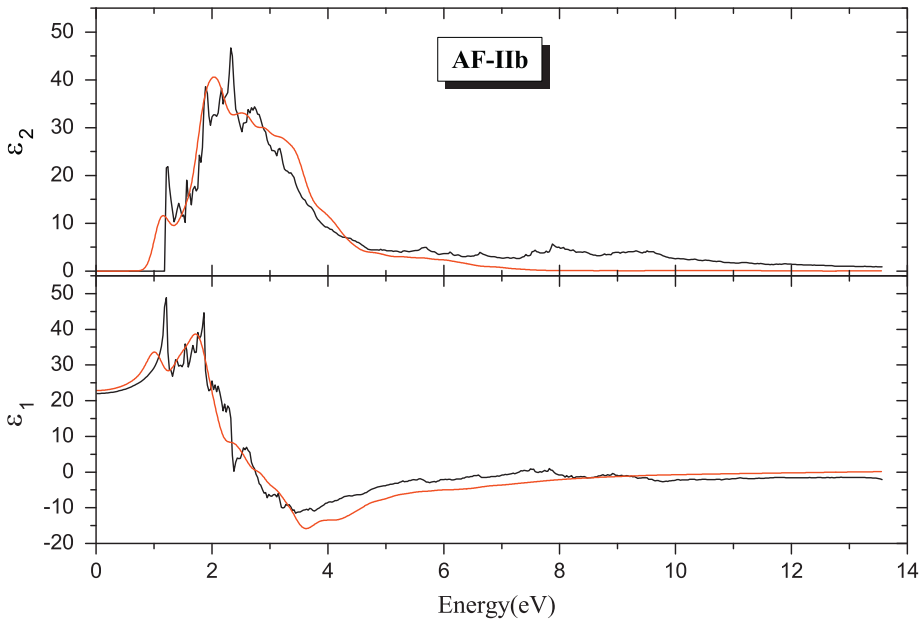

Fig. 6. The calculated real and imaginary part of dielectric function for AF-IIb phases, FP- LAPW(black line) and PP-PW (red line). (For interpretation of the references to color in this figure legend, the reader is referred to the web version of this article.)

calculated in the high symmetry directions of the Brillouin zone, is given in Fig. 4. The valence band maximum (VBM) is located at *X* point for AF-IIb, whereas the conduction band minimum (CBM) is located at ($L\Gamma$) directions. The energy gap obtained from FP-LAPW approach is 0.07 eV, while that obtained from PP-PW calculations is 0.28 eV. In

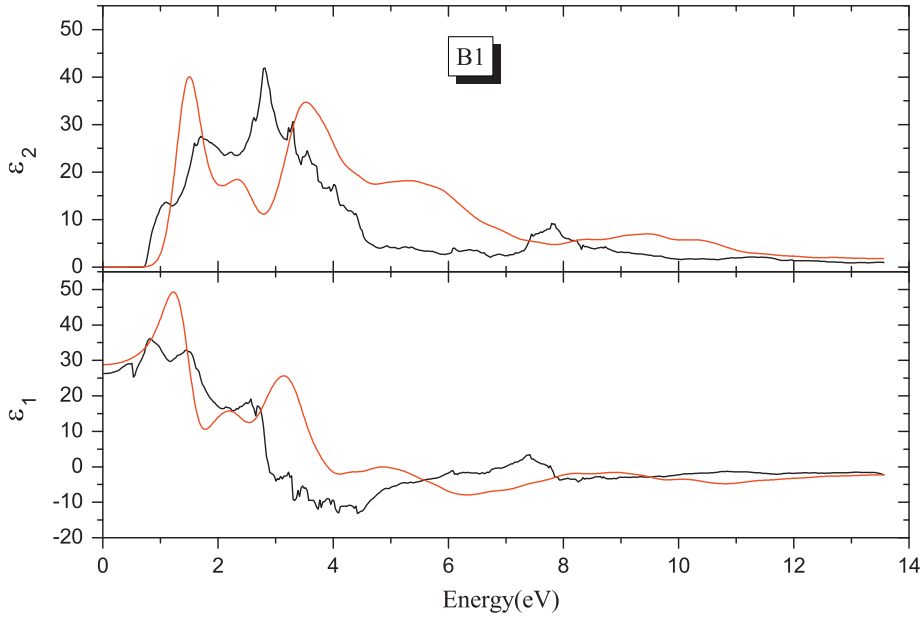

Fig. 7. The calculated real and imaginary part of dielectric function for B1 phases, FP-LAPW(black line) and PP-PW (red line). (For interpretation of the references to color in this figure legend, the reader is referred to the web version of this article.)

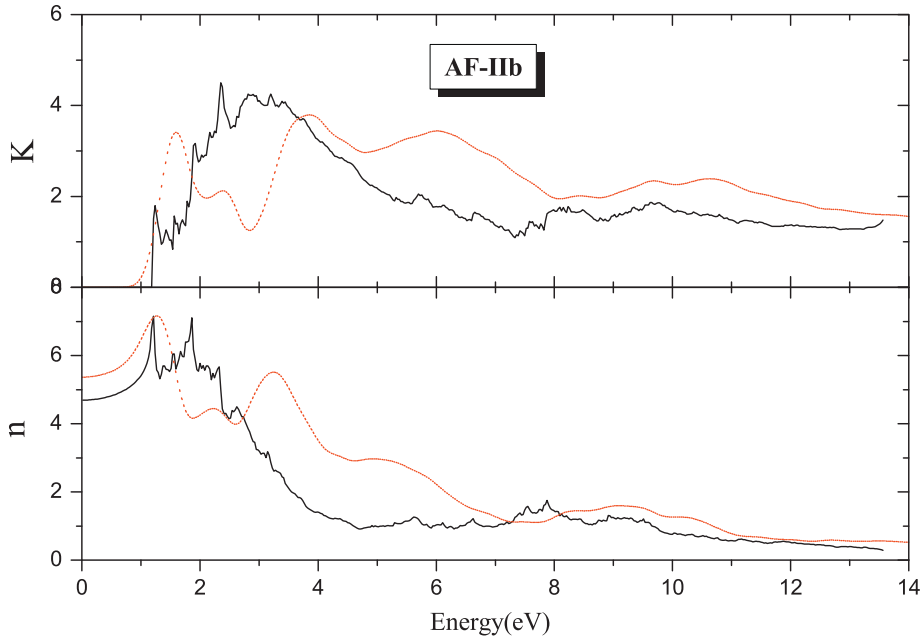

Fig. 8. Calculated refractive index $n(w)$ and extinction coefficient for AF-IIb phases, FP-LAPW(black line) and PP-PW (red line). (For interpretation of the references to color in this figure legend, the reader is referred to the web version of this article.)

the case of B1 phase the valence band maximum (VBM) is located at W point, whereas the conduction band minimum (CBM) is located at (ΓX) directions leads to a pseudogap of about −0.8 eV when using FP-LAPW and −1.41 eV from PP-PW method. Total and partial densities of states of this compound are given in Fig. 5. Note that for AF-IIb the DOS can be divided into three parts, at lower energy where we find the contribution of Sb p and S s states; the second part is from −6 eV to 0 eV that is mainly derived from Ag p and S p states, the third part which is beyond the Fermi level, where the contribution is due to S p and Ag s states. For the B1 phase, a few Sb s states occur at lower energies. The contribution of Ag d states appear from −6 eV to 0 eV and the conduction band is mainly derived from Sb p and S p states.

3.3. Optical properties.

The dielectric function, refractive index and extinction coefficients at the equilibrium lattice constant were calculated using both FP-LAPW and PP-PW approaches.

In Figs. 6 and 7 we present the dielectric function of $AgSbS_2$ as calculated by FP-LAPW and PP-PW methods for AF-IIb and B1 phases, respectively. For energies up to

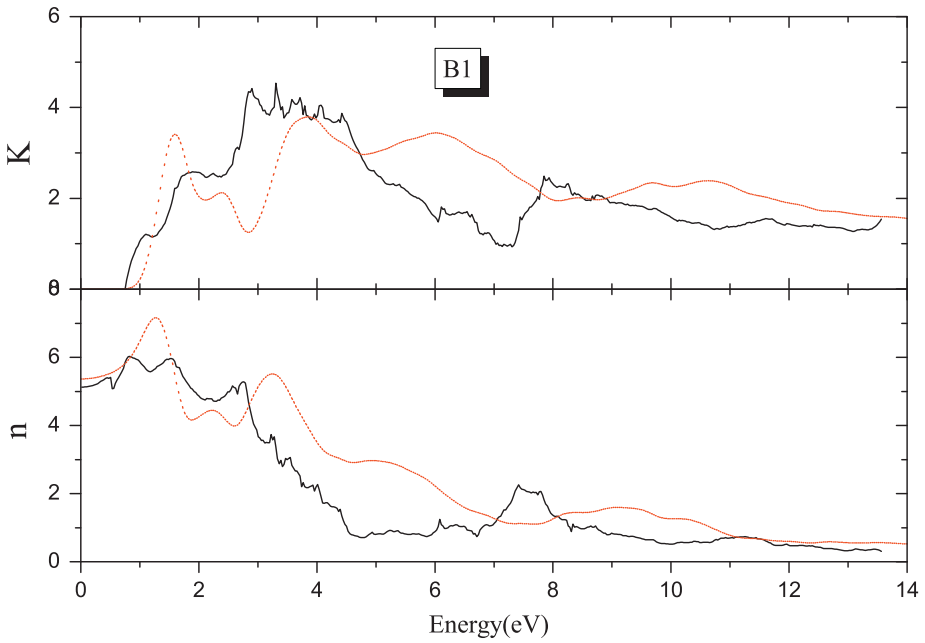

Fig. 9. Calculated refractive index $n(w)$ and extinction coefficient for B1 phases, FP-LAPW(black line) and PP-PW (red line). (For interpretation of the references to color in this figure legend, the reader is referred to the web version of this article.)

14 eV, based on our calculated band structure it would be worthwhile to identify the interband transitions that are responsible for the structure in $\varepsilon_2(\omega)$. Our analysis of the $\varepsilon_2(\omega)$ spectra shows that the threshold energy (first critical point) of the dielectric function occurs at about 0.7 eV for B1 phase (Fig. 7), while in AF-IIb phase (Fig. 7) it occurs at 1.19 eV and 0.8 eV for FP-LAPW and PP-PW methods, respectively. These points are mainly coming from the electron transition from the S 3s (VB) to Ag 5p (CB) orbitals. We note that in AF-IIb phase, $\varepsilon_2(\omega)$ shows a peak located at 2.3 eV and 2.02 eV for FP-LAPW and PP-PW methods, respectively. This point is mainly derived from the transition from Sb5s (VB) to S3p (CB) orbitals. In the case of B1 phase, the peak is located at 2.83 eV for the FP-LAPW method and 1.5 eV for the PP-PW method. This point is mainly derived from the transition from Ag 4d (VB) to Sb 3p (CB) orbitals. The behavior of $\varepsilon_1(\omega)$ seems to be rather similar to that of $\varepsilon_2(\omega)$. Below the reststrahlen region in the optical spectra, the real part of the dielectric function asymptotically approaches the static or low-frequency dielectric constant ε_0. In the present contribution, the calculated static dielectric constant ε_0 in AF-IIb phase is found to be about 22.075 and 22.85 using FP-LAPW and PP-PW methods, respectively. In case of B1 phase, the calculated static dielectric constant ε_0 is found to be 26.31 and 28.99 using FP-LAPW and PP-PW methods, respectively.

The refractive index and the extinction coefficient are displayed in Figs. 8 and 9 for AF-IIb and B1 phases, respectively. Note that the calculated data show clear peaks originating from the excitonic transitions at the E_0 edges. The strongest peaks in $n(\omega)$ spectra are related mainly to the 2D exciton transition (E_1) [35]. Using the FP-LAPW method, the static refractive index $n(0)$ is found to be 4.695 for AF-IIb phase and 5.125 for B1 phase. These values differ largely from those of 5.39 and 5.355 obtained using PP-PW method for AF-IIb and B1 phases, respectively. In the absence of both experimental and theoretical data of the dielectric function, refractive index and extinction coefficients for the material of interest, to the best of our knowledge, no comment can be ascribed to the accuracy of the two used methods and hence our results may serve only for a reference.

4. Conclusion

Using the FP-LAPW and PP-PW methods where the exchange–correlation potential was calculated with the frame of GGA, we have analyzed the structural, electronic and optical properties of $AgSbS_2$ for both AF-IIb and B1 phases. The calculated equilibrium lattice constant of the material of interest is found to be in good agreement with experiment when the FP-LAPW method is used whereas a slight deviation from experiment was found when using the PP-PW method. We found that the material in question is a semiconductor that has an indirect band gap $X\rightarrow(\Gamma L)$ energy. The band structure of the $AgSbS_2$ material showed an intermetallic behavior in the B1 phase suggesting that the materila of interest is a semimetal in this phase. The dielectric function, refractive index, extinction coefficient were calculated for radiations up to 14 eV. The critical point structure of the frequency dependence complex dielectric function was investigated and analyzed to identify the optical transitions. Linear optical properties such as the dynamic dielectric function from 0 up to14 eV were discussed.

References

[1] A. Jeyaraman, P.D. Dernier, H.M. Kasper, R.G. Maines, High Temperatures High Pressures 9 (1977) 97.

[2] C. Carlone, D. Olego, A. Jeyaraman, M. Cordona, Physical Review B 22 (1980) 3877.
[3] J. Gonalez, M. Quintero, C. Rincon, Physical Review B 45 (1992) 7022.
[4] T. Sakunthala, P. Akilesh, K. Arora, Physical Review B 53 (1996) 15667.
[5] L. Roa, J.C. Chervin, A. Chevy, M. Davila, P. Grima, J. Gonzalez, Physica Status Solidi (B) 198 (1996) 99.
[6] C. Wood, Reports on Progress in Physics 51 (1988) 459.
[7] G.D. Mahan, Solid State Physics 51 (1998) 81.
[8] K.-F. Hsu, S. Loo, F. Guo, W. Chen, J.S. Dyck, C. Uher, T. Hogan, E.K. Polychroniadis, M.G. Kanatzidis, Science 303 (2004) 818.
[9] L.G. Voinova, V.A. Bazakutsa, S.A. Dembovskii, L.G. Lisovskii, E.P. Sokol, C.T. Kantser, Izvestiya Vysshikh Uchebnykh Zavedenij Fizika 5 (1971) 154.
[10] A.S. Tsytko, S.A. Dembovskii, I.I. Ezhik, V.A. Bazakutsa, Izvestiya Vysshikh Uchebnykh Zavedenij Fizika 12 (1969) 154.
[11] I. Kelleher, S.A.T. Redfern, R.A.D. Pattrick, Mineralogical Magazine 60 (1996) 393.
[12] J.V. Smith, J.J. Pluth, S.-X Han, Mineralogical Magazine 61 (1997). 671 and references therein.
[13] E Quarez, K.F Hsu, R. Pcionek, N Frangis, E.K Polychroniadis, M. G. Kanatzidis, Journal of the American Chemical Society 127 (2005) 9177.
[14] S. Ravhi Kumar, L. Andrew, Cornelius Eunja Kim, Yongrong Shen, S. Yoneda, Changfeng Chen, F. Malcolm Nicol, Physical Review B 72 (2005) 060101(R).
[15] Khang Hoang, S.D. Mahanti, James R. Salvador, Mercouri G. Kanatzidis, Physics Letters 93 (2007) 156403.
[16] J.L. Shay, J.H. Wernick, Ternary Chalcopyrite Semiconductors: Growth, Electronic Properties and Applications_Pergamon Press, New York, 1975.
[17] A.M. Gaber, J.R. Tuttle, D.S. Albin, A.L. Tennaant, M.A. Contreras, in: R. Noufi, H.L. Ullal (Eds.), AIP Conference Proceedings of the 12th NREL Photovoltaic Program Review, 306, American Institute of Physics, New York, 1994, p. 59.
[18] H.S. Soliman, A.D. Abdel-Hadey, E. Ibrahim, Journal of Physics: Condensed Matter 10 (1998) 847.
[19] P. Blaha, K. Schwarz, P. Sorantin, S.B. Trickey, Computer Physics Communications 59 (1990) 399.
[20] P. Hohenberg, W. Kohn, Physical Review B 36 (1964) 864.
[21] P. Blaha, K. Schwarz, G.K.H. Medsen, D. Kvasnicka, J. Luitz, An augmented plane wave local orbitals program for calculating crystal properties, in: Karlheinz Schwartz (Ed.), WIEN2k, Techn. Universitad, Wien, Austria, 2001.
[22] J.P. Perdew, K. Burke, M. Ernzerhof, Physical Review Letters 77 (1996) 3865.
[23] H.J. Monkhorst, J.D. Pack, Physical Review B 13 (1976) 5188.
[24] M. Alouani, J.M. Wills, Physical Review B 54 (1996) 2487.
[25] L. Klienman, D.M. Bylander, Physical Review Letters 48 (1982) 1425.
[26] M.D. Segall, P.J.D. Lindan, M.J. Probert, C.J. Pickard, P.J. Hasnip, S.J. Clark, M.C. Payne, Journal of Physics: Condensed Matter 14 (2002) 2717.
[27] T.H. Fischer, J. Almlof, Journal of Physical Chemistry 96 (1992) 9768.
[28] F.D. Murnaghan, Proceedings of the National Academy of Sciences USA 30 (1944) 244.
[29] S. Geller, J.H. Wernick, Acta Crystallographica 12 (1959) 46–54.
[30] S. Saib, N. Bouarissa, Solid-State Electronics 50 (2006) 763.
[31] S. Zerroug, F. Ali Sahraoui, N. Bouarissa, European Physical Journal B 57 (2007) 9.
[32] GÖkhan GÖkoğlu, Physica B 405 (2010) 2162–2165.
[33] J. Winterlik, G.H. Fecher, A. Thomas, C. Felser, Physical Review B 79 (2009) 064508.
[34] A. Gueddim, N. Bouarissa, A. Villesuzanne, Physica Scripta 80 (2009) 055702.
[35] A. Gueddim, S. Zerroug, N. Bouarissa, Journal of Luminescence 135 (2013) 243.